IEEE Access
Multidisciplinary | Rapid Review | Open Access Journal

Received October 25, 2019, accepted November 8, 2019, date of publication November 14, 2019, date of current version November 27, 2019.

Digital Object Identifier 10.1109/ACCESS.2019.2953479

On Droop Control of Energy-Constrained Battery Energy Storage Systems for Grid Frequency Regulation

JAE WOONG SHIM[1], (Member, IEEE), GREGOR VERBI[2], (Senior Member, IEEE), HEEJIN KIM[3], (Member, IEEE), AND KYEON HUR[3], (Senior Member, IEEE)

[1]Department of Energy Engineering, Inje University, Gimhae 50834, South Korea
[2]School of Electrical and Information Engineering, The University of Sydney, Sydney, NSW 2000, Australia
[3]School of Electronic and Electrical Engineering, Yonsei University, Seoul 03722, South Korea

Corresponding author: Kyeon Hur (khur@yonsei.ac.kr)

This work was supported in part by the Korea Electric Power Corporation under Grant R17XA05-4, and in part by the "Human Resources Program in Energy Technology" of the Korea Institute of Energy Technology Evaluation and Planning (KETEP), granted financial resource from the Ministry of Trade, Industry and Energy, Republic of Korea, under Grant 20194030202420.

ABSTRACT This paper proposes the droop control algorithm for multiple distributed Battery Energy Storage Systems (ESS) with their state of charge (SOC) feedback, shown to be effective in providing grid services while managing the SOC of the ESS. By extending the mathematical links between the ESS SOC and power dynamics for frequency regulation, this paper elaborates on how the proposed scheme integrates multiple ESS into the load frequency control and the ESS effectively augments the functional roles of the incumbent generators. The control performance for a group of ESS in grid operations is evaluated and characterized by using metrics such as the cut-off frequency and settling time, and the initial and final value theorems. Theoretical insights and practical issues are discussed. Various numerical examples and case studies for a simplified Australian network with high penetration of renewables demonstrate the validity and efficacy of the proposed method.

INDEX TERMS Energy storage system (ESS), frequency regulation, reserve, droop control, state of charge (SOC), energy feedback, SOC management.

I. INTRODUCTION

The introduction of an energy storage system (ESS) changes the paradigm of a power system, and gradually plays an important role in the frequency regulation (FR) of the system to balance the energy generation and consumption. Numerous ESS installation projects are being conducted by various utilities such as PJM [1], NYISO [2], ERCOT [3], KEPCO [4], etc. [5]–[8]. Sandia National Laboratories has made a significant effort in this regard through collaboration with utility companies and reported the multifaceted benefits through studies on a DOE ESS program [9]–[12]. Moreover, FERC has recognized the importance of an ESS and enacted the laws 'Order 755' and 'Order 784' to encourage ESS installation for utilities [13], as well as the revised regulations 'Order 819' related to the sale of a primary frequency response (PFR) service, permitting the sale of PFR services based on market-based rates. These laws were enacted to foster competition in the sale of PFR services and expand the ancillary services market [14]. Conventional frequency coordination is well-constructed in the following order: inertia response, governor response, and automatic generation control (AGC) [15]–[18] and this should be co-operative and coordinated with FR ESS for effective frequency regulation. As future grid might be operated with low system inertia weakening frequency stability due to a high penetration of renewable energy sources (RES), the role of ESS can become even more important for the reinforcement of the stability for upcoming grid. Against this backdrop, various studies on ESS applications have been carried out. SOC feedback method for ESS droop control has been analyzed in the frequency domain [19], [20]. Droop control with a certain amount of power for an ESS was conceptually introduced [21]. The effectiveness of the droop set point adjustment as a load frequency control (LFC)

The associate editor coordinating the review of this manuscript and approving it for publication was Fabio Massaro.

has also been illuminated [22]. The management of an SOC to obtain potential reserves using penalty functions has been described [23]. Adaptively adjusting the droop rate has also been researched for a vehicle-to-grid (V2G) system in consideration of SOC [24], [25]. A micro-grid consisting of PV/ESS has also been explored [26]. DC grid droop control for a matching SOC has been illuminated [27], [28], and an ESS application in a multi-terminal HVDC was introduced [29]. Research on SOC control for a hybrid ESS [20], [30], and hierarchical control of the SOC in a DC grid, have been carried out [31]. Several studies have attempted to employ a droop method with SOC management and feedback [24], [25], [31]–[35]. Some of the research presents sensitivity studies in different grid conditions [36]. However, studies on an ESS aggregation method for frequency control coordination are still in the development stage. Reference [19] proposed a droop and SOC feedback method for the harmonious integration of multiple ESSs. Whereas the principles and benefits of the droop control with SOC feedback for an ESS are presented in [19], this previous study focused on frequency domain analysis of the ESS operation and control with SOC feedback method.

In this study, we propose the ESS aggregation method based on the droop control with SOC feedback method and analyze this using several indicators, thus academic contributions of the research can be summarized as follows:

- Mathematical formulation of the droop control with offset based on SOC feedback
- ESS aggregation method in coherent area (ESS size and the number of parallel ESS change)
- Theoretical insight of ESS from various viewpoints (the response time, the spectrum of compensation, and operating point change)
- Effectiveness of ESS for the system with low inertia constant.

ESS aggregation using the droop control with SOC feedback are suitable for the existing frequency regulation (FR) by providing assistance to the inertia and governor actions, as can be seen in Fig. 1, which shows that an ESS recovers the SOC during the AGC regulation period, and that the energy for SOC recovery is supported by generators with AGC.

Herein, we demonstrate that the ESS aggregation using the droop control with SOC feedback are suitable for the existing frequency regulation (FR) by providing assistance to the inertia and governor actions, as can be seen in Fig. 1, which shows that an ESS recovers the SOC during the AGC regulation period, and that the energy for SOC recovery is supported by generators with AGC. The remainder of this paper is organized as follows: Section II describes the droop control with SOC feedback method, Section III explains the theoretical operation mechanism, Section IV presents the frequency stability using the droop control with SOC feedback method, Section V shows the case of renewable integration, and in Section VI, we provide some concluding remarks regarding this research.

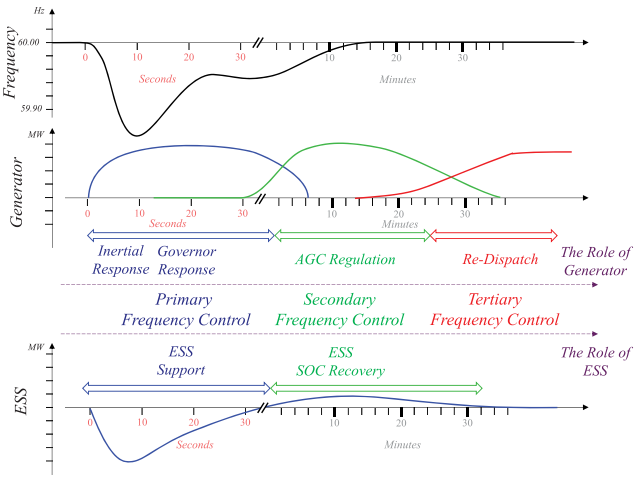

FIGURE 1. General information of frequency regulation with ESS and existing generation system: Coordinated roles of the ESS and incumbent generators along the operational time frame.

II. DROOP CONTROL AND SOC FEEDBACK METHOD

A. SOC CALCULATION OF ESS

The SOC of a battery is often calculated by integrating the current [37], [38]. Since this relation is between current and SOC, it does not directly express the relationship between battery power and SOC. By assuming that the internal voltage of the battery is constant, the current is proportional to the power. The SOC of the ESS can then be directly calculated using the energy concept by integrating power and the transfer function can also be derived as shown in (1) and (2), respectively. The dynamics of SOC and Power of ESS is used for establishing a link between the SOC and grid frequency change.

$$SOC(t) = SOC_0 + \frac{1}{E \cdot h} \int_{t_0}^{t} P_{\mathrm{ESS}}(t)dt \tag{1}$$

$$\frac{\Delta SOC_0(s)}{\Delta P_{\mathrm{ESS}}(s)} = \frac{1}{E \cdot h} \cdot \frac{1}{s} = \frac{1}{K_{\mathrm{E}} s} \tag{2}$$

where SOC_0 is the initial SOC, E is the nominal capacity of the battery (MWh), h indicates a factor to change hours seconds ($h = 3600$), P_{ESS} is the battery power (MW), $\Delta SOC_0(t) = SOC(t) - SOC_0$, and $K_{\mathrm{E}} = E \cdot h$ [MW·sec] is the energy of the ESS in joule (ESS capacity based on the number of seconds).

B. DYNAMICS OF SOC IN RESPONSE TO FREQUENCY CHANGE

Droop control aims to share the burden among ESSs and generators for a frequency regulation. The droop rate (R_{ESS}) in (3) denotes when the frequency (Δf) deviates, and the supporting units offer the power. The different droop rates (R_{ESS}) will provide different degrees of power in response to the frequency deviation (Δf) in (3).

The relation between power and SOC in (2) and droop equation in (3) can be combined and expressed as the relation

between frequency variation and SOC in (4).

$$\Delta P_{\mathrm{ESS}}(t) = \frac{1}{R_{\mathrm{ESS}}} \cdot \Delta f(t) \tag{3}$$

$$\frac{\Delta SOC(s)}{\Delta f(s)} = \frac{1}{R_{\mathrm{ESS}}} \cdot \frac{1}{E \cdot h} \cdot \frac{1}{s} = \frac{1}{R_{\mathrm{ESS}} K_{\mathrm{E}} s} \tag{4}$$

C. THEORETICAL REPRESENTATION OF DROOP CONTROL WITH SOC FEEDBACK

The droop control with SOC feedback method is developed as an energy management method for FR ESS application.

In this method, for the management of the SOC level, we subtract the frequency offset (f_{ofs}) from the frequency deviation as in (5) for the ESS power calculation [19]. The frequency offset is a feedback value converted from the SOC to the frequency unit. So, frequency offset (f_{ofs}) is calculated by multiplying SOC with K_{f} as in (6).

The parameter K_{f} plays the most important role in this method, which is the conversion factor between SOC and grid frequency for SOC feedback as in (7).

$$\Delta P_{\mathrm{ESS}}(t) = \frac{1}{R_{\mathrm{ESS}}}(\Delta f(t) - f_{\mathrm{ofs}}(t)) \tag{5}$$

$$f_{\mathrm{ofs}}(t) = \Delta SOC(t) \cdot K_{\mathrm{f}} \tag{6}$$

$$K_{\mathrm{f}} = (f_{\mathrm{ofs,max}} - f_{\mathrm{ofs,min}})/SOC_{\mathrm{tot}} \tag{7}$$

where $\Delta f = f - f_{\mathrm{n}}$, $\Delta SOC = SOC - SOC_{\mathrm{cen}}$, ΔP_{ESS} is the charging power of the ESS, Δf can be both the frequency deviation and the reference of the frequency offset, f_{ofs} is the frequency offset, ΔSOC is the SOC deviation from the central value, K_{f} [Hz/%] is the allocation of the SOC range to the frequency compensation range, $f_{\mathrm{ofs,max}}$ is the maximum of the frequency compensation, $f_{\mathrm{ofs,min}}$ is the minimum of the frequency compensation, and SOC_{tot} is the SOC control range such as zero to 100.

D. MECHANISM OF DROOP CONTROL WITH SOC FEEDBACK METHOD

The droop control with SOC feedback method is an ESS frequency regulation method considering the SOC as SOC_{ref} proportionately changes by following frequency deviation for management of the ESS energy (SOC) according to the degree of frequency variation.

Fig. 2 from (2), (5), and (6) shows the droop with SOC feedback method from two perspectives: (a) frequency offset feedback and (b) SOC feedback. We added K_{f} for a frequency offset feedback from the SOC in Fig. 2(a), whereas $1/R_{\mathrm{ESS}}$ and K_{E} are the existing droop controller and SOC calculation, respectively. To calculate $\Delta SOC_{\mathrm{ref}}$ in (8), SOC_{cen} is assigned for a nominal frequency f_{n}, implying that, when frequency (f) reaches the nominal frequency (60 Hz), SOC_{ref} reaches the central value (50%), linked through K_{f}, as in (8).

$$\begin{aligned}\Delta SOC_{\mathrm{ref}}(t) &= SOC_{\mathrm{ref}}(t) - SOC_{\mathrm{cen}} \\ &= (f(t) - f_{\mathrm{n}})/K_{\mathrm{f}} = \Delta f(t)/K_{\mathrm{f}}\end{aligned} \tag{8}$$

$$\begin{aligned}\Delta f(t) - f_{\mathrm{ofs}}(t) &= \Delta f(t) - \Delta SOC(t) \cdot K_{\mathrm{f}} \\ &= (\Delta SOC_{\mathrm{ref}}(t) - \Delta SOC)(t) \cdot K_{\mathrm{f}}\end{aligned} \tag{9}$$

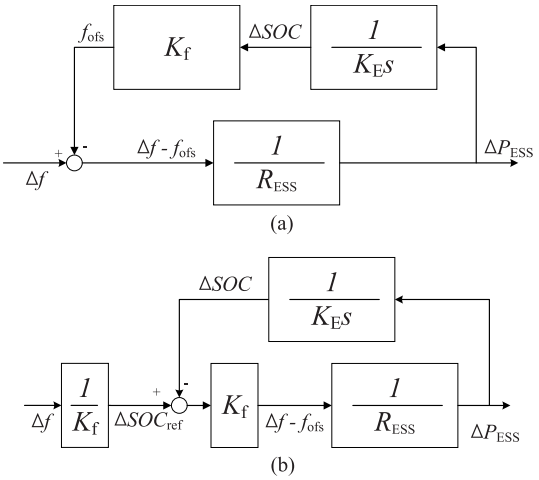

FIGURE 2. Block diagram of droop control with SOC feedback method from two different perspectives: (a) frequency offset and (b) SOC feedback points of view.

where f_{n} indicates the nominal frequency, f is system frequency, SOC is the measured SOC, SOC_{cen} is the center of SOC, e.g. 50% when SOC_{tot} is 100%, f_{n} is nominal frequency, SOC_{ref} is SOC reference, and $\Delta SOC_{\mathrm{ref}}$ is a deviation of SOC reference from the central SOC.

Fig. 2(a) shows that the frequency deviation is the reference and the frequency offset is a feedback signal. Thus, the frequency offset intends to follow the frequency deviation. For example, if a frequency deviation occurs (Δf), the droop input ($\Delta f - f_{\mathrm{ofs}}$) proportionally changes the power ΔP, and determines the SOC (ΔSOC). Then, the change in ΔSOC creates a change in f_{ofs}; as a result, $\Delta f - f_{\mathrm{ofs}}$ will be zero in the long term.

Fig. 2(b) shows the droop with SOC feedback method from the SOC perspective. In this figure, when a frequency deviation occurs, the change in Δf leads to a change in the SOC reference ($\Delta SOC_{\mathrm{ref}}$) in (8). Then, this will lead the change of the power ΔP, based on the value between SOC reference ($\Delta SOC_{\mathrm{ref}}$) and the measured SOC ($\Delta SOC$), and this results in a change of ΔSOC. Finally, $\Delta SOC_{\mathrm{ref}} - \Delta SOC$ will be zero in the long term. It is important to note that the droop with SOC feedback method can be implemented in two ways.

The droop with SOC feedback method enables the SOC to proportionally follow the frequency deviation, which indicates that a slight frequency deviation results in a slight SOC change, whereas a large frequency deviation leads to large change in SOC. To summarize, the droop control with SOC feedback method manages the SOC automatically and supports the system frequency as the ESS has limited energy.

E. OPERATIONAL BEHAVIOR OF METHODOLOGY

For the behavior explanation, we compared two ESSs with different levels of SOC for two frequency deviation cases, in Fig. 3, and the frequency deviations are assumed as constant values for a solid understanding.

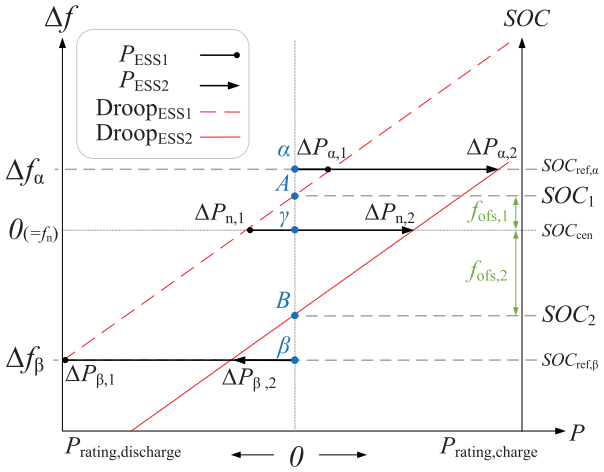

FIGURE 3. Illustration of droop control with SOC feedback method; subtracting the frequency offset from the frequency deviation.

The relationship between two y-axes (SOC and Δf) are directly connected through K_f in Fig. 3 as in (6)-(9); thus, SOC_1 and SOC_2 turn into the frequency offsets ($f_{\mathrm{ofs},1}$ and $f_{\mathrm{ofs},2}$) added to the droop slope.

The frequency deviation Δf_α and Δf_β ($SOC_{\mathrm{ref},\alpha}$ and $SOC_{\mathrm{ref},\beta}$) are linked to points α and β, and $f_{\mathrm{ofs},1}$ and $f_{\mathrm{ofs},2}$ (SOC_1 and SOC_2) are connected with the points A and B. Namely, α, β, and γ are dependent on the external power system, and A and B are dependent on the internal ESS system.

If the frequency (Δf_α) deviates, ESS_1 and ESS_2 absorb power as $\Delta P_{\alpha,1}$ and $\Delta P_{\alpha,2}$, respectively, indicating when a grid has excessive power and the frequency increases, ESS_1 with a higher SOC_1 absorbs less power $\Delta P_{\alpha,1}$, and ESS_2 with a lower SOC_2 absorbs higher power $\Delta P_{\alpha,2}$, because ESS_1 has a lower chargeable energy capacity than ESS_2.

As a consequence, the power charge makes the SOCs (SOC_1 and SOC_2) move toward $SOC_{\mathrm{ref},\alpha}$; in other words, $f_{\mathrm{ofs},1}$ and $f_{\mathrm{ofs},2}$ move toward Δf_α. Consequently, points A and B are tracking point α.

In another case, when the system requires more power generation or support, the frequency drops as Δf_β. ESS_1 with a higher SOC_1 discharges higher power $\Delta P_{\beta,1}$, and ESS_2 with a lower SOC_2 releases less power $\Delta P_{\beta,2}$, as the ESS with a higher SOC_1 has higher capacity with dischargeable energy than ESS_2 with a lower SOC_2 (lower dischargeable energy). In this operation, both points A and B are tracking point β.

In this sense, we need to note that ESS_1 starts with high power ($\Delta P_{\beta,1}$) and SOC_1 changes quickly; however, when SOC_1 of ESS_1 moves to nearly $\Delta P_{\beta,2}$, ESS_1 discharges low power and SOC_1 changes more slowly.

III. THEORETICAL DISCUSSION OF AGGREGATION METHOD FOR DROOP CONTROL WITH SOC FEEDBACK

This section intends to shed a clearer light on the behaviors of this method through a mathematical explanation. A block diagram of a power system using a ESS with this method is illustrated in Fig. 4 without a communication delay.

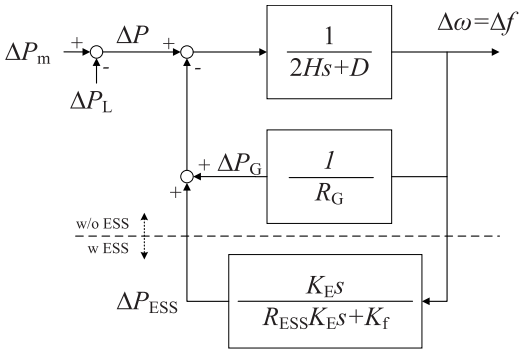

FIGURE 4. Block diagram of ESS application with SOC feedback on the system.

A. SOC RESPONSE OF ESS WITH DROOP CONTROL WITH SOC FEEDBACK

This method provides the mathematical insight using transfer functions by the frequency characteristics.

The transfer function of the SOC response can be derived from equations in (10), (2), (5), and (6), resulting in (11), which indicates that the SOC deviates, such as the first-order filter in response to the frequency deviation.

Equation (11) is a transfer function to observe the relation between ΔSOC and Δf in Fig. 2(a).

This transfer function shows that SOC proportionally changes by following grid frequency as first order function with time constant $(R_{\mathrm{ESS}} \cdot K_{\mathrm{E}})/K_{\mathrm{f}}$ and gain $(1/K_{\mathrm{f}})$.

$$\Delta SOC(s) = \frac{1}{K_{\mathrm{E}} \cdot s}\left(\frac{1}{R_{\mathrm{ESS}}}\Delta f(s) - \Delta SOC(s) \cdot K_{\mathrm{f}}\right) \quad (10)$$

$$\frac{\Delta SOC(s)}{\Delta f(s)} = \frac{1}{K_{\mathrm{f}} + R_{\mathrm{ESS}} K_{\mathrm{E}} s} \quad (11)$$

B. POWER RESPONSE OF DROOP CONTROL WITH SOC FEEDBACK ESS

The equation of the power response (12) can be derived from (2), (5), and (6), which can be formulated into (13) as a transfer function, and becomes a type of high-pass filter (HPF), particularly the washout filter form with the gain $1/R_{\mathrm{ESS}}$ and the time constant $(R_{\mathrm{ESS}} \cdot K_{\mathrm{E}})/K_{\mathrm{f}}$.

$$\Delta P_{\mathrm{ESS}}(s) = \frac{1}{R_{\mathrm{ESS}}}\left(\Delta f(s) - \frac{\Delta P_{\mathrm{ESS}}}{K_{\mathrm{E}} s} \cdot K_{\mathrm{f}}\right) \quad (12)$$

$$\frac{\Delta P_{\mathrm{ESS}}(s)}{\Delta f(s)} = \frac{K_{\mathrm{E}} s}{R_{\mathrm{ESS}} K_{\mathrm{E}} s + K_{\mathrm{f}}} \quad (13)$$

This transfer function shows that ESS power only compensates high frequency band (fast fluctuation) of grid frequency, and ESS does not compensate low frequency band (long-term grid frequency deviation) for the management of ESS energy.

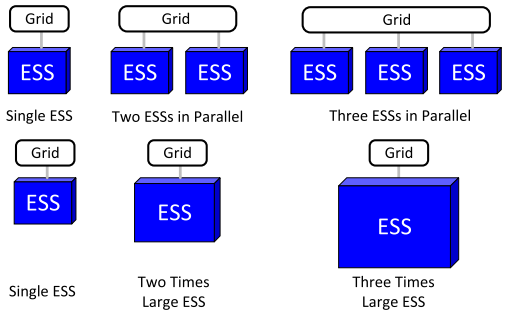

FIGURE 5. Conceptial illustration of the different number of ESS in parallel and different size of ESS.

C. ESS AGGREGATION ACCORDING TO ESS SIZE AND DROOP RATE

When the ESS is installed on the power system, various types of installations can be expressed in the form of the change in size or parallel connection as in Fig. 5. This types of installation (parallel connection and size change) can be expressed using the change of droop rate (R) and ESS size (K_{E}).

If the distributed ESSs is installed on the power system, these ESSs are considered as parallel connection and the equivalent droop rate which is the factor of contribution to the power system can be expressed as in (14) if droop rate of ESS (R_{ESS}) are identical.

$$R_{\mathrm{ESS,eq}} = \frac{1}{\frac{1}{R_{\mathrm{ESS,1}}} + \cdots \frac{1}{R_{\mathrm{ESS,y}}}} = \frac{R_{\mathrm{ESS}}}{Y} \tag{14}$$

where $R_{\mathrm{ESS,eq}}$ is equivalent droop rate of the ESSs, $R_{\mathrm{ESS,y}}$ is the droop rate of the y^{th} ESSs in pu, R_{ESS} is the droop rate of single ESSs in pu, and Y is the number of parallel ESS.

In case larger number of ESS installed on the power system, simplified and aggregated ESS model can help effective simulation and decrease computation burden if it has identical performance and contribution.

For the ESS aggregation, the converters with droop control in parallel can be expressed as R/Y which is parallel converter numbers. The size of ESS can be expressed as $X \cdot K_{\mathrm{E}}$ which is multiple number of ESS. The transfer function of ESS aggregation model can be derived as (15) and (16) as can be shown in Fig. 6 based on the condition above with (11) and (13).

$$\frac{\Delta SOC(s)}{\Delta f(s)} = \frac{1}{K_{\mathrm{f}}} \frac{1}{(\frac{X \cdot R_{\mathrm{ESS}} K_{\mathrm{E}}}{Y \cdot K_{\mathrm{f}}})s + 1} \tag{15}$$

$$\frac{\Delta P_{\mathrm{ESS}}(s)}{\Delta f(s)} = \frac{1}{R_{\mathrm{ESS}}} \frac{(\frac{X \cdot R_{\mathrm{ESS}} K_{\mathrm{E}}}{Y \cdot K_{\mathrm{f}}})s}{(\frac{X \cdot R_{\mathrm{ESS}} K_{\mathrm{E}}}{Y \cdot K_{\mathrm{f}}})s + 1} \tag{16}$$

where ΔP_{ESS} is the ESS power, Δf is the frequency deviation, ΔSOC is the SOC deviation from the central value, K_{f} [Hz/%] is the allocation of the SOC range to the frequency compensation range, R_{ESS} is droop rate of ESS, X is X times larger ESS sizes, Y parallel numbers of ESS, and

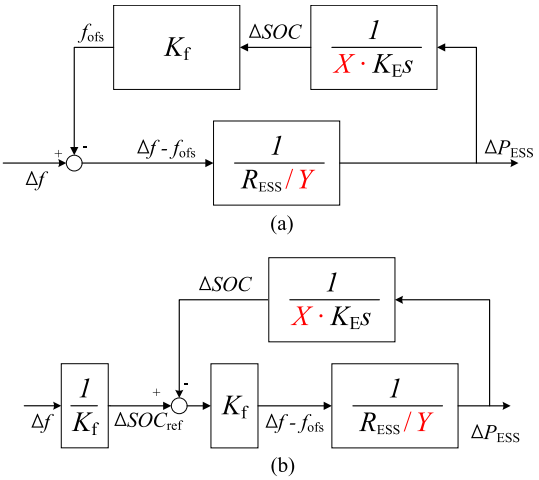

FIGURE 6. Block diagram of ESS aggregation from two different perspectives: (a) frequency offset and (b) SOC feedback points of view.

TABLE 1. Response characteristics of ESS.

	Cases	X	Y	Gain (db)	Cut-off Freq.	Settling Time
Case 1	Single ESS	1	1	5 (13.98)	7.3683 e-04	972
Case 2	Two ESS in parallel	2	2	10 (20)	7.3683 e-04	972
Case 3	Two Times Larger ESS	2	1	5 (13.98)	3.6841 e-04	1944

$K_{\mathrm{E}} = E \cdot h$ [MW·sec] is the energy of the ESS in joule (ESS capacity based on the number of seconds).

1) RESPONSE CHARACTERISTICS OF CONDITIONAL CHANGES IN FR ESS WITH SOC FEEDBACK

For the case study, three cases are developed to examine the impact of change in ESS sizes (X) and parallel ESS numbers (Y) on the control performance. In case of ESS size change, we assume that converter rating is identical.

Equation (17) indicates the cut-off frequency of the ESS transfer function at (13). Equation (18) stands for the settling time ($\pm$ error $< 2\%$) from (19) in [40]. Table 1 presents the gain (3), cut-off frequency (17), and settling time (18) in each case for a different ESS sizes (X) and parallel ESS numbers (Y).

$$f_{\mathrm{c}} = \frac{1}{2\pi} \left| \frac{K_{\mathrm{f}}}{(R_{\mathrm{ESS}}/Y)(K_{\mathrm{E}} \cdot X)} \right| \tag{17}$$

$$t_{\mathrm{s,ESS}} = \frac{3.9(R_{\mathrm{ESS}}/Y)(K_{\mathrm{E}} \cdot X)}{K_{\mathrm{f}}} \tag{18}$$

$$t_{\mathrm{s,ESS}} = 3.9\tau \tag{19}$$

where f_{c} is the cut-off frequency of the ESS, Y is the parallel number of ESSs, X is the total size of the ESSs compared to

[1]The droop rate of the ESS is considered with the system rating, and the frequency and SOC are the pu (60 Hz and 100% respectively). The system base and rating are 1 GW. A single ESS size is 500 kWh.

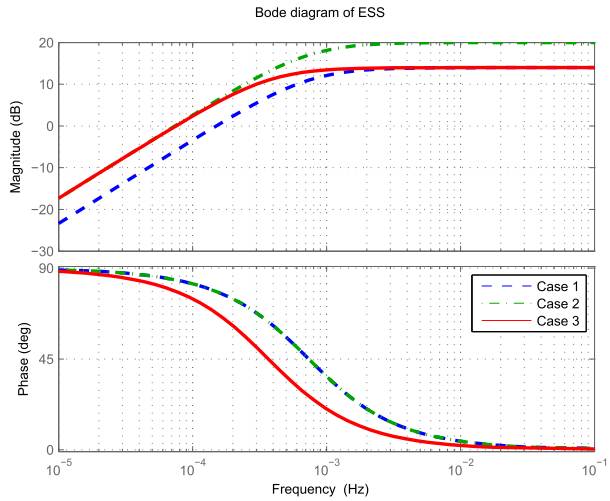

FIGURE 7. Bode plot of transfer function of droop with SOC feedback in (13): Case 1, single ESS; Case 2, two ESSs; and Case 3, two-times larger ESS.

a single ESS size, $t_{s,ESS}$ is the settling time of the ESS, t_s is the settling time (2%), and τ is the time constant.

To select the parameters, we must consider that K_f is for the SOC range to the frequency range in (10), the initial value of the ESS power can be determined based on the droop rate, as in (3), and the size of the ESS (K_E) can be determined for the coverage of the frequency using the cut-off frequency in (18) and (19), respectively.

First, 'Single ESS' in Case 1 compares one ESS on one converter with the other cases, in which the gain, cut-off frequency, and settling time are listed as in Table 1.

Second, in Case 2 for 'two ESSs in parallel,' the droop rate (R_{ESS}) becomes half of the single ESS by (21), and the total size of ESS (K_E) becomes twice that of a single ESS. As a consequence, the cut-off frequency and settling time remain the same because X/Y is '1' in (17) and (18); however, the gain (Y/R_{ESS}) increases twice in Case 1, as shown in Table 1, owing to the decrease in droop rate by half based on (21). In this sense, the distributed ESSs can independently regulate the frequency together in a decentralized manner.

Third, 'two-times larger ESS,' namely, Case 3, indicates a case with a double-sized ESS (X) without a parallel ESS (Y). As a result, the settling time increases as indicated in Table 1, and the cut-off frequency decreases to lower the frequency band. The ESS with higher energy can support the system for a longer time, although the initial value starts with an identical gain as in Case 1.

2) ANALYSIS OF FR ESS WITH SOC FEEDBACK ON BODE PLOT AND TIME DOMAIN

Figs. 7 and 8 compare the three cases in Table 1 using the bode plot and time frame of the transfer function of (13).

In the bode plot in Fig. 7, the gain of Case 2 increases two-fold compared to Case 1, thus the value of Case 2 on the time frame is magnified to twice that of Case 1, as shown in Fig. 8. The cut-off frequency and settling time of Cases 1 and 2 are

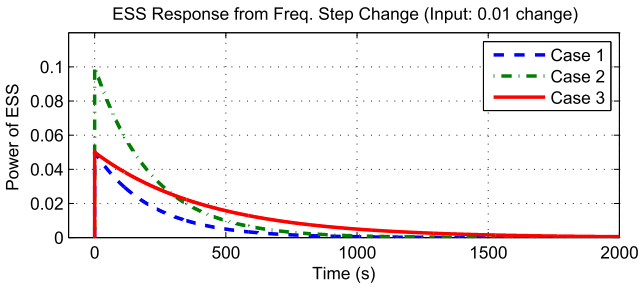

FIGURE 8. Response of droop with SOC feedback method: Case 1, single ESS; Case 2, two ESSs; Case 3, two-times larger ESS.

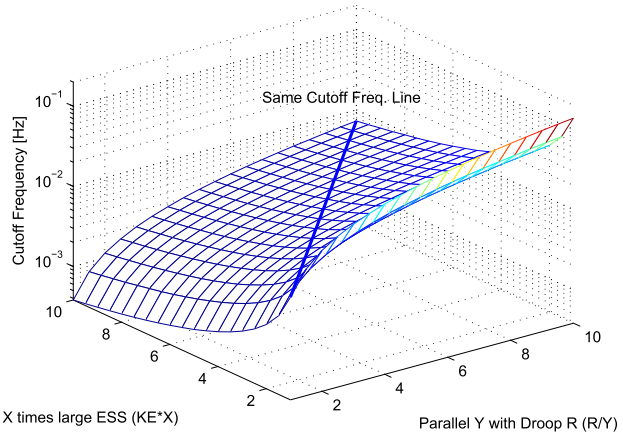

FIGURE 9. Cut-off frequency in terms of the total ESS size (X) and parallel ESS numbers (Y).

identical, as indicated in Table 1. Case 3 covers the lower frequency band without a gain change, as shown in Fig. 7, and the initial value of Case 3 is the same as in Case 1 but provides a longer support, which shows that Case 3 covers a lower frequency band.

Fig. 9 displays the interrelationship between $K_E \cdot X$ and R_{ESS}/Y concerning the cut-off frequency of the case studies. Fig. 9 indicates that when the parallel ESS number (Y) increases (the droop rate (R_{ESS}/Y) decreases), the cut-off frequency increases; however, when the total ESS energy ($K_E \cdot X$) increases, the cut-off frequency decreases according to (17). Furthermore, we should note that the cut-off frequency is constantly maintained where X and Y match.

D. FREQUENCY RESPONSE OF POWER SYSTEM WITH DROOP CONTROL WITH SOC FEEDBACK

1) INITIAL VALUE OF FREQUENCY WITH ESS USING SOC FEEDBACK

The characteristic of the composite regulation in terms of aggregated droop control is introduced in Kundur's book [39]. The initial and final points are intimately linked with the composite droop rate (R_{eq}). Immediately after the step change, the initial status of the ESS can approximate that Laplace operator goes to infinity. Subsequently, the initial value is the inverse droop rate of ESS as in (20).

$$\frac{\Delta P(s)}{\Delta f(s)} = \lim_{s\to\infty} \frac{K_E s}{R_{ESS} K_E s + K_f} \cdot s \cdot \frac{1}{s} \simeq \frac{1}{R_{ESS}} \tag{20}$$

If the distributed ESSs can support the system, the initial support starts with the equivalent droop rate of parallel ESSs ($R_{\mathrm{ESS,eq}}$) and generators together (R_{eq}), as in (21). The frequency deviation supported by both ESSs and generators can be described as in (22) with equivalent droop control.

$$R_{\mathrm{eq}} = \frac{1}{\frac{1}{R_{\mathrm{ESS,eq}}} + (\frac{1}{R_{\mathrm{G},1}} + \cdots \frac{1}{R_{\mathrm{G,m}}})} \tag{21}$$

$$\Delta f(s) = \frac{1}{D + 1/R_{\mathrm{eq}}} \cdot \Delta P(s) \tag{22}$$

where R_{eq} is the equivalent droop rate of the system including ESSs and generators, $R_{\mathrm{ESS,eq}}$ is equivalent droop rate of the ESSs, $R_{\mathrm{G,m}}$ is the droop rate of m^{th} generators in the pu, and D is the load damping component.

2) FINAL VALUE OF FREQUENCY WITH/WITHOUT FR ESS WITH SOC FEEDBACK

Based on the final value theorem, we can examine the tendency of governor control with FR ESS with SOC feedback. We should observe the SOC management from the ESS when the frequency deviation continuously occurs without the AGC. The final frequency value has a Laplace form applying $s = 0$ as in (23), [40].

$$\lim_{t\to\infty} g(t) = \lim_{\mathrm{s}\to 0} sG(s) \tag{23}$$

where $\mathcal{L}[g(t)]$=$G(s)$, $g(t)$ is a function of time, and $G(s)$ is a function of the Laplace formation.

The total transfer functions without/with ESS are formulated as in (24) and (25), respectively, from Fig. 4. A system event is assumed as a step function of the power deviation ($\Delta P(s)/s$). As a result, both (24) and (25) are converged into the same result in (26). The power support of the ESS diminishes for a long term, as in (26), and only the support of the generators remains because the factor of the ESS does not remain in (26).

$$\Delta f_{\mathrm{ss}}(s) = \lim_{\mathrm{s}\to 0} \frac{s \cdot \Delta P(s)/s}{2Hs + D + 1/R_{\mathrm{G}}} \tag{24}$$

$$\Delta f_{\mathrm{ss}}(s) = \lim_{\mathrm{s}\to 0} \frac{s \cdot \Delta P(s)/s}{(2Hs + D + 1/R_{\mathrm{G}}) + (K_{\mathrm{E}} s/(R_{\mathrm{ESS}} K_{\mathrm{E}} s + K_{\mathrm{f}}))} \tag{25}$$

$$\Delta f(0) = \frac{1}{D + 1/R_{\mathrm{G}}} \cdot \Delta P(0) \tag{26}$$

where Δf_{ss} is the steady state of a frequency deviation, R_{G} is the equivalent droop rate of the generators, H is an inertia constant, D is the load damping component, ΔP is a deviation of power in pu, R_{ESS} is the droop rate of all ESSs, K_{E} [MW·sec] the ESS capacity in joule, and K_{f} [Hz/%] is the coefficient for allocation between the SOC and frequency compensation range.

3) GRAPHICAL DESCRIPTION OF INITIAL AND FINAL POINTS

The initial and final points (22) and (26) are illustrated as Fig. 10 based on net frequency sensitivity theory in Kundur's book [39]. The initial compensation from the ESS

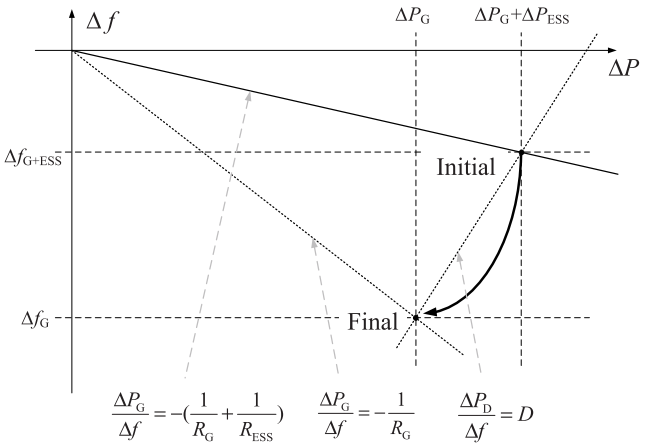

FIGURE 10. Net frequency sensitivity for initial and final values of frequency with ESS with SOC feedback, composite governor, and load characteristics.

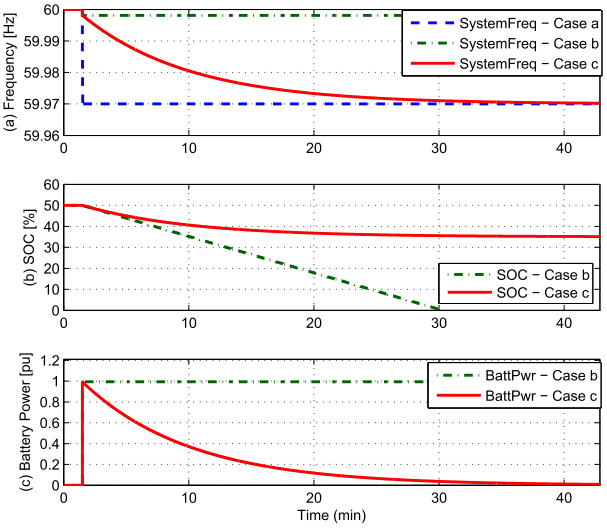

FIGURE 11. Outline of frequency deviation: Case A, without an ESS; Case B, with droop control; and Case C, with the droop with SOC feedback method.

and the generator power ($\Delta P_{\mathrm{G}} + \Delta P_{\mathrm{ESS}}$) is shown in the x-axis of Fig. 10; consequently, the frequency slightly deviates as $\Delta f_{\mathrm{G+ESS}}$. In contrast, the long-term compensation is not provided by the ESS due to the SOC management, and only generators provide the power (ΔP_{G}) without ESS support in long term. Subsequently, the frequency deviation moves to the final point in Fig. 10. The frequency from the initial to the final points moves as a first-order function.

4) VERIFICATION OF INITIAL AND FINAL POINTS

In this section, three case studies are established to verify the initial and final calculations based on Fig. 10, namely, Case A is with only generators with droop control (governor), Case B is with ESS using droop control (w/o SOC feedback); and Case C is with ESS using droop control and SOC feedback. In these case studies, the frequency drops and remains constantly, as in Fig. 11, after the contingency at 50 [s].

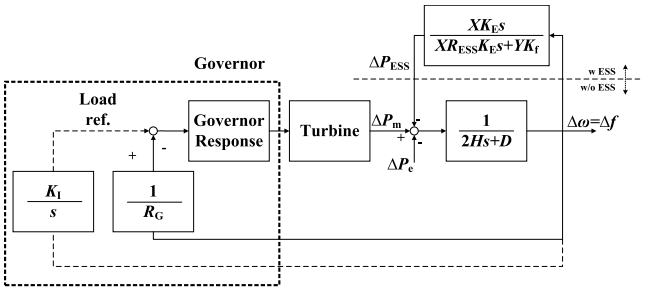

FIGURE 12. Block diagram of system for frequency stability study.

Case A indicates the deepest frequency deviation among the cases owing to the droop control from the governor in Fig. 11(a), because the ESS does not support the system.

Case B, which illustrates an ESS without SOC feedback, offers power continuously, as shown in Fig. 11(c), which highly reduces the frequency deviation in Fig. 11(a) and linearly decreases the SOC in Fig. 11(b). However, because the ESS has limited energy, the time of the power support is also limited owing to a lack of ESS energy, as shown in Fig. 11(b).

Case C, as illustrated in Fig. 11(c), shows that the power of the ESS changes, similar to a high-pass filtered value, and the frequency deviates, similar to a low-pass filtered value, which create a compromises between the frequency support and SOC management.

The initial power of the ESS equals the power in Case B; however, the amount of power gradually decreases to zero such as with a high-pass filtered value, as shown in Fig. 11(c) and as indicated in (13). The change in SOC settles to a single point, similar to a low-pass filtered value, as indicated in Fig. 11(b) and presented in (11).

Consequently, the frequency deviation starts with the full support of the ESS, as in Case B, but finishes without ESS support, as in Case A. These characteristics are of particular importance to understand the behavior of this method and compromisingly seek frequency support and energy management.

IV. INTEGRATION OF ESS WITH SOC FEEDBACK ON POWER SYSTEM

To verify the efficacy of FR ESS with SOC feedback on the frequency stability, the system is formulated using a turbine and governor based on the reheat steam turbine generator model [39], as indicated in Fig. 12 and Table 2. The transfer functions of the governor and turbine are indicated in (27) and (28), respectively. FR ESS with SOC feedback in Fig. 12 supports the power (ΔP_{ESS}), and the electrical power (ΔP_e) includes fluctuations of renewable generation and contingencies from the load, line, and other factors.

$$G_{Gov}(s) = \frac{1}{1+sT_G} \tag{27}$$

$$G_{Tur}(s) = \frac{1+sF_{HP}T_{RH}}{(1+sT_{CH})(1+sT_{RH})} \tag{28}$$

TABLE 2. Parameters for frequency stability[1].

Variable	H	K_E	R_G	D	K_f	K_I	R_{ESS}
Value	5	1.8	0.05	0.01	0.1 /60	20	0.2

TABLE 3. The parameters of parallel ESS (Y) and ESS Size (X).

Parameters	X	Y
Single ESS	1	1
Five Times Larger Size (TLS) ESSs	5	1
Ten Times Larger Size (TLS) ESSs	10	1
Single ESS	1	1
Five ESSs in Parallel	5	5
Ten ESSs in Parallel	10	10

A. FREQUENCY REGULATION WITH GENERATOR DROOP CONTROL

This chapter aims to observe the characteristics of the droop control with SOC feedback method, and thus we assume that the frequency constantly deviates.

1) INFLUENCE OF ESS SIZE

For the ESS aggregation model, the case study is carried out with changing ESS capacity. In this case, the droop rate is fixed and the ESS capacity is changed, in other words, in connection to one converter, a large ESS or a small ESS is installed. Since the droop rate is constant, the initial power compensation of ESS in response to frequency deviation is identical although the size of ESS is different as can be shown in Fig. 13. As capacity of ESS changes, the ability to maintain SOC also changes, namely, the small ESS capacity is having difficulties in maintaining the SOC. However, the larger ESS capacity is with the ability to maintain the SOC and to compensate for longer periods of time.

From the view point of the parameter, when the ESS size (K_E) increases without the change in droop rate (R_{ESS}), the initial power support is not influenced because the initial power depends only on ($1/R_{ESS}$), as indicated in Fig. 13(a). The increase in the size of the ESS (K_E) changes the supporting time of the ESS power, as shown in Fig. 13(b), which means that the cut-off frequency decreases and the settling time increases. In addition, the change in SOC has also different characteristics, in Fig. 13(c).

2) INFLUENCE OF ESS NUMBERS

To determine the differences among the ESS numbers, we increase the parallel ESS numbers by identically changing X and Y in (17) and (18). The cut-off frequency and time constant of the ESS are fixed because the multiplication between the joules of the ESS (K_E) and the droop rate (R_{ESS}) in (17) and (18) remains constant. However, the differences in the compensated frequency in accordance with the different conditions in each case lead to the different responses of the ESS power and SOC.

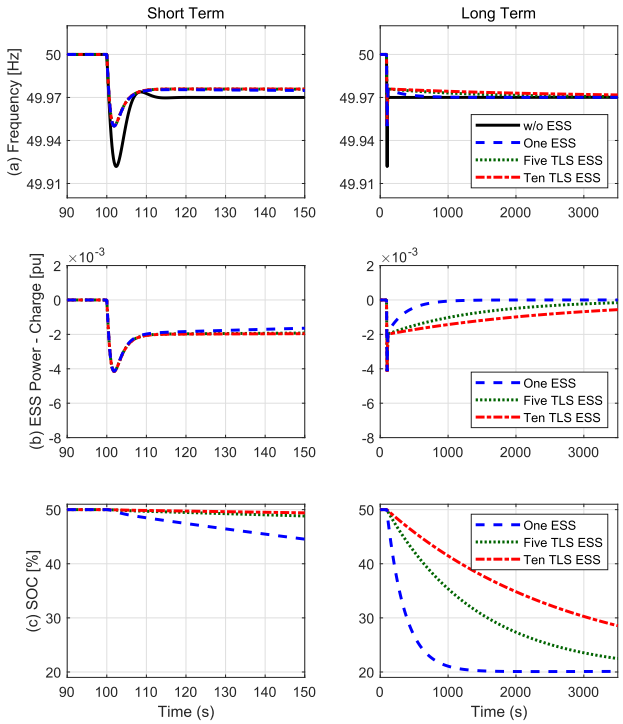

FIGURE 13. The response of ESS aggregation model - ESS size change with a constant droop rate: w/o ESS, single ESS, five-times larger size (TLS) ESS, and ten-times larger size (TLS) ESS.

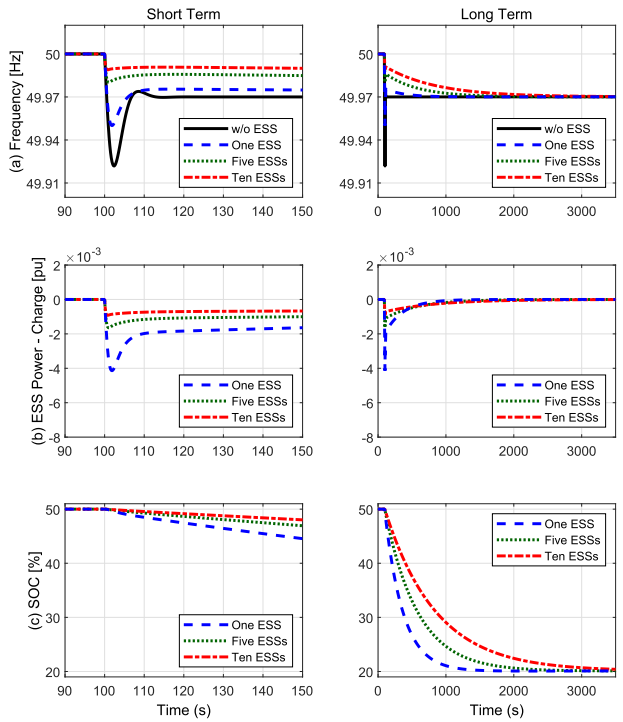

FIGURE 14. The response of ESS aggregation model - the number of parallel ESS change (both of ESS size and droop rate) : w/o ESS, single ESS, five ESSs, and ten ESSs.

Fig. 14 compares one, five, and ten ESSs in parallel. The figure shows that the supporting power from the plural ESSs reduces the frequency deviation in the short term and changes the settling time in the long term as the number of ESSs increases, as indicated in Fig. 14(a). The initial power from each ESS in the short term, as shown in Fig. 14(b), is reduced owing to the increased ESS numbers and the responses have differences in the long term. Because of these different power responses, the responses of the SOC also have differences. The results in this section indicate that the larger number of ESSs connected in a parallel manner can be effective for the short-term frequency stability, because a fleet of ESSs provides high power.

B. FREQUENCY REGULATION WITH LOAD FREQUENCY CONTROL

Because the characteristics of the ESS can be defined as a limited energy and faster action, whereas that of the generator can be defined as long-lasting energy and a slower action, the ESS and generator can cooperate with each other to cover the drawbacks of the others and to offer mutual compensation.

1) ROLE OF ESS FREQUENCY COORDINATION

A reduced number of conventional generators is the root of two problems: the reduced inertial energy and the reduced aggregated droop slope of the system. Both problems are located in the primary response, namely, the fastest section in the frequency control sequence, as shown in Fig. 1. The role of each ESS in the existing frequency compensation procedure should be clearly defined for providing a well-balanced ancillary service. Thus, we define the role of the ESS for the existing FR based on the droop control with SOC feedback method characteristics.

- Primary control: The static reserve (ESS) supports the inertial energy and governor control.
- Secondary control: The generators take charge of the frequency recovery; subsequently, the ESS recovers the SOC.

2) COORDINATED GRID FREQUENCY CONTROL BETWEEN GENERATOR AND FR ESS WITH SOC FEEDBACK

Mutual compensation between generators (slower action and large energy) and ESSs (faster action and limited energy) is available with the characteristics of the droop control with SOC feedback method.

The support from a FR ESS with SOC feedback is placed in primary reserve because this method operates with generators owing to the droop characteristics. In secondary reserve, a re-dispatch and AGC action eliminate the steady state error of the frequency; meanwhile, a frequency recovery leads to an SOC recovery. More precisely, the LFC operation drives the frequency to a nominal value, allowing the generators to provide an enormous amount of energy within a few minutes. Meanwhile, the ESS recovers the center of the SOC (SOC_{cen}), as indicated in Fig. 2(b) and Fig. 3, when the frequency returns to the nominal value (f_{n}). Namely, in primary reserve, the ESS takes the responsibility of supporting the governor action. In secondary reserve, the generator takes the responsibility of the ancillary service through the LFC, and the ESS should launch

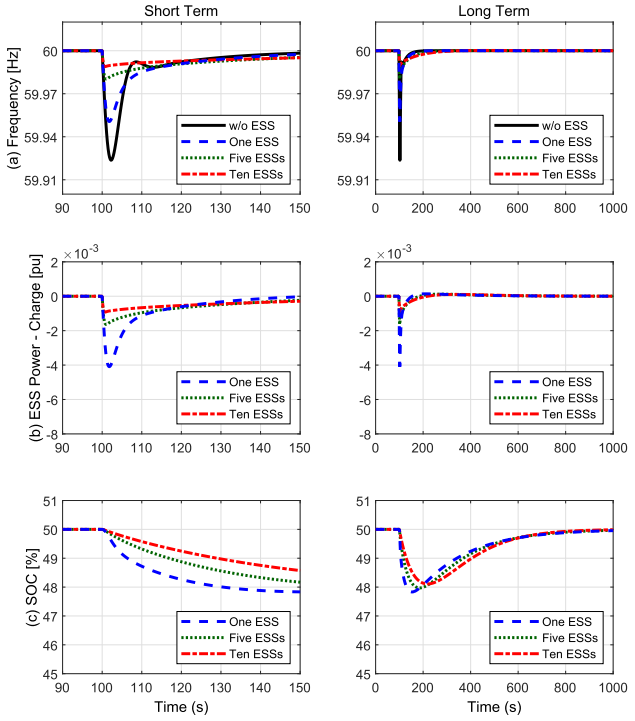

FIGURE 15. The response of ESS aggregation model - the number of parallel ESS change under AGC operation (short term, primary control; long term, secondary control).

the energy management. Thus, the droop control with SOC feedback method can be explained as a negative LFC.

Fig. 15 visually presents a harmonious operation between the ESSs and generators. The fleet of ESSs supports the power for the short term, as indicated in Fig. 15(b), and lessens the frequency deviation, as shown in Fig. 15(a). For the longer term, the LFC operation is carried out to recover the frequency to a nominal value, and FR ESS with SOC feedback manages its energy by adjusting the SOC to the center value shown in Fig. 15(c).

V. EFFECTIVENESS OF ESS ON POWER SYSTEM WITH LOW INERTIA

A. SIMULATION ENVIRONMENTS

The power network is designed based on the Australian Future Grid Scenario [41], [42], as can be seen in Fig. 16. In this system, most of the concentrating solar thermal power Plants (CSPs) are located in the central area of Australia, and wind power plants (WPPs) are spread along the coast, especially in the south of Australia.

Because fewer conventional generators are in operation, the inertia constant of the network is reduced from the original system to the cases shown in Table 4, and the increase in the penetration level may increase the vulnerability of frequency stability. The aggregated inertia constants within the coherent generation areas can be calculated through (29).

$$H_{\text{tot}} = \sum_{i=1}^{n_{\text{gen}}} H_i n_i \frac{S_i}{S_{\text{base}}} \tag{29}$$

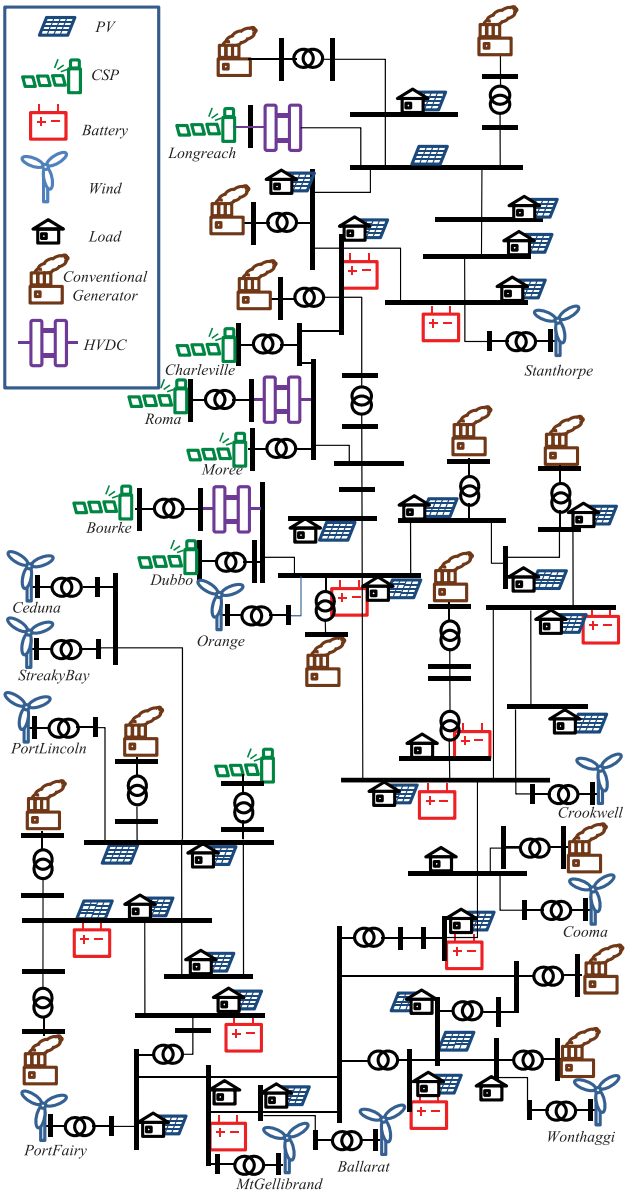

FIGURE 16. The 14 generator model (simplified Australian system) based on the Australian Future Grid Scenario.

where n_{gen} is the number of generators, n_{i} indicates the number of i_{th} generators, S_{i} is the rating of the i_{th} generator; H_{i} stands for the inertia of the i_{th} generator; and S_{base} is the base of the system.

In this system, we assume that all ESSs are owned by the utility for service reliability and predictability. The ESS operation method is solely for the frequency regulation with the droop control with SOC feedback method.

B. RENEWABLE INTEGRATION

In this case, practical PV and WPP data are applied to the system, as shown in Fig. 17(a) and (b), and the extremely fluctuating renewable energy sources (RESs) increase the power imbalance and frequency fluctuation problem; moreover, the reduced inertia constant can alleviate the existing problem.

TABLE 4. System condition for bulk system.

	Original Model	Case 1	Case 2
Generation of Conventional Units	22,212.9MW	13,984.7MW	13,984.7MW
Generation of RES Units	0MW	8,230MW	8,230MW
Inertia Constant(s) (S_{base}:1GW)	93.01 s	56.01 s	56.01 s
Penetration level (%)	0	32.18	32.18
Static Reserve (ESS)	-	-	220 MW

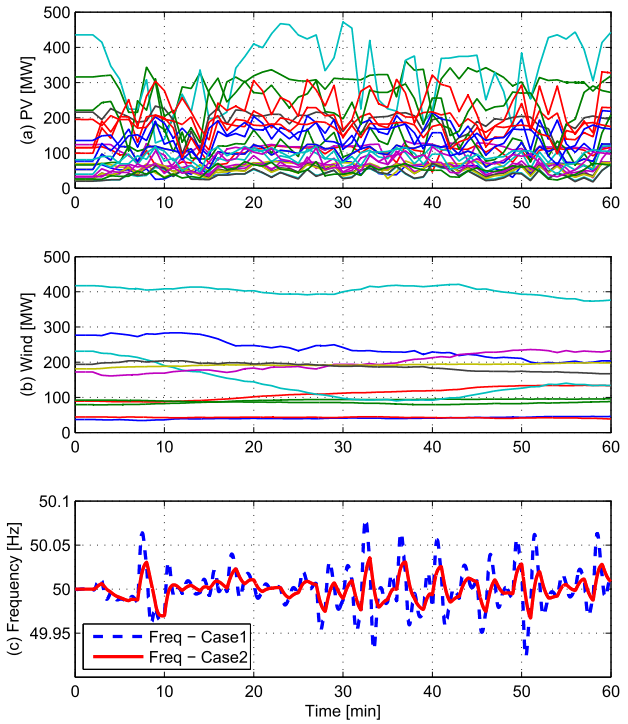

FIGURE 17. Renewable fluctuation case on 14 generator model: (a) PV power, (b) wind power, and (c) system frequency.

The governor and AGC actions cannot eliminate the high-frequency band of system frequency; thus, if FR ESS with SOC feedback covers higher frequency, the fluctuation of the system frequency becomes much smoother.

The system frequency with and without an ESS is presented in Fig. 17(c). The contribution of the ESS in Fig. 17(c) provides evidence of the explanation in Figs. 7 and (13); the ESS eliminates and takes responsibility of the high-frequency band; consequently, the fluctuations of the frequency deviation decrease.

VI. CONCLUSION

This paper expanded on the droop control with SOC feedback method for grid services by clarifying the mathematical links among the functional components via transfer functions, and underlying mechanism though performance analysis based on industry-friendly metrics. We thoroughly examined the performance by changing the size and number of participating ESS with SOC feedback method: The scheme incorporates successfully multiple ESS and manages the SOC to a desire level. In terms of power system operation at high renewable penetration, we investigated the response of the ESS on the governor system with droop and load frequency control operation cases. The research outcome of the study may lead to various promising applications for future research and application in terms of EV, power smoothing, multi-functional applications. As ascertained from the studies above, the ESS with the proposed scheme effectively compensates the frequency in harmony with incumbent sources for frequency regulation services while maintaining the desired SOC.

REFERENCES

[1] "To determine the effectiveness of the AGC in controlling fast and conventional resources in the PJM frequency regulation market," KEMA, Chalfont, PA, USA, KERMIT Study Tech. Rep., Dec. 2011.
[2] D. Allen, C. Brown, J. Hickey, V. Le, and R. Safuto, "Energy storage in the New York electricity market," New York Independ. Syst. Operator (NYISO), Rensselaer, NY, USA, Tech. Rep., 2010.
[3] "Future ancillary services in ERCOT," Electr. Rel. Council Texas, Austin, TX, USA, Tech. Rep., Sep. 2013.
[4] W. Hur, Y. Moon, K. Shin, W. Kim, S. Nam, and K. Park, "Economic value of Li-ion energy storage system in frequency regulation application from utility firm's perspective in Korea," *Energies*, vol. 8, no. 6, pp. 5000–5017, May 2015.
[5] M. van der Hoeven, "Technology roadmap: Energy storage," Int. Energy Agency (IEA), Paris, France, Tech. Rep., Mar. 2014.
[6] Sandia National Laboratories. *The DOE Global Energy Storage Database*. Accessed: Jul. 2019. [Online]. Available: http://www.energystorageexchange.org/
[7] M. Atanacio, R. Fioravanti, W. Katzenstein, and K. Vu, "Emmission ii study of advanced storage used for frequency regulation," Sandia Nat. Lab., Sandia Negotiation, Albuquerque, NM, USA, Tech. Rep., 96362, Dec. 2011.
[8] Y. Zhang, V. Gevorgian, C. Wang, X. Lei, E. Chou, R. Yang, Q. Li, and L. Jiang, "Grid-level application of electrical energy storage: Example use cases in the United States and China," *IEEE Power Energy Mag.*, vol. 15, no. 5, pp. 51–58, Sep./Oct. 2017.
[9] J. Eyer and G. Corey, "Energy storage for the electricity grid: Benefits and market potential assessment guide," Sandia Nat. Lab., Albuquerque, NM, USA, Tech. Rep. 2010-0815, 2010.
[10] S. M. Schoenung and W. V. Hassenzahl, "Long- vs. Short-term energy storage technologies analysis: A life-cycle cost study, a study for the doe energy storage systems program," Sandia Nat. Lab., Albuquerque, NM, USA Tech. Rep. 2003-2783, Aug. 2003.
[11] R. Baxter, "Energy storage financing: Performance impacts on project financing," Sandia Nat. Lab., Albuquerque, NM, USA, Tech. Rep. 2018-10110, Sep. 2018.
[12] A. A. Akhil, G. Huff, A. B. Currier, B. C. Kaun, D. M. Rastler, S. B. Chen, A. L. Cotter, D. T. Bradshaw, and W. D. Gauntlett, "DOE/EPRI electricity storage handbook in collaboration with NRECA," Sandia Nat. Lab., Albuquerque, NM, USA, Tech. Rep. SAND2013-5131, Jan. 2015.
[13] C. A. LaFleur, P. D. Moeller, J. R. Norris, and T. Clark, "Third-party provision of ancillary services; accounting and financial reporting for new electric storage technologies: 18 CFR Parts 35, 101 and 141," Federal Energy Regulatory Commission (FERC), Washington, DC., USA, Tech. Rep., Jul. 2013.
[14] N. C. Bay, C. A. LaFleur, T. Clark, and C. D. Honorable, "Third-party provision of primary frequency response service: 18 CFR Part 35. Docket no. Rm15-2-000," Federal Energy Regulatory Commission (FERC), Washington, D.C., USA, Tech. Rep., Nov. 2015.
[15] G. Zhang, "EPRI power systems dynamics tutorial," Electr. Power Res. Inst., Palo Alto, CA, USA, Tech. Rep. 1016042, Jul. 2009.
[16] M. Yao, R. R. Shoults, and R. Kelm, "AGC logic based on NERC's new control performance standard and disturbance control standard," *IEEE Trans. Power Syst.*, vol. 15, no. 2, pp. 852–857, May 2000.
[17] "Frequency response standard background document," North Amer. Electr. Rel. Corp. (NERC), Atlanta, GA, USA, Tech. Rep., Nov. 2012.
[18] R. Quint and D. Ramasubramanian, "Impacts of droop and deadband on generator performance and frequency control," in *Proc. IEEE Power & Energy Soc. Gen. Meeting*, Jul. 2017, pp. 1–5.

[19] J. W. Shim, G. Verbi , N. Zhang, and K. Hur, "Harmonious integration of faster-acting energy storage systems into frequency control reserves in power grid with high renewable generation," *IEEE Trans. Power Syst.*, vol. 33, no. 6, pp. 6193–6205, Nov. 2018.
[20] J. W. Shim, "The impact of large-scale renewable energy on grid small-signal and frequency stability: Modelling, analysis, and control," Ph.D. dissertation, School Electron. Elect. Eng., Yonsei Univ., Seoul, South Korea, School Elect. Inf. Eng., Univ. Sydney, Sydney, NSW, Australia, Jul. 2016.
[21] C. A. Hill, M. C. Such, D. Chen, J. Gonzalez, and W. M. Grady, "Battery energy storage for enabling integration of distributed solar power generation," *IEEE Trans. Smart Grid*, vol. 3, no. 2, pp. 850–857, Jun. 2012.
[22] I.-Y. Chung, W. Liu, D. A. Cartes, E. G. Collins, and S. I. Moon, "Control methods of inverter-interfaced distributed generators in a microgrid system," *IEEE Trans. Ind. Appl.*, vol. 46, no. 3, pp. 1078–1088, May/Jun. 2010.
[23] J. Dang, J. Seuss, L. Suneja, and R. G. Harley, "SOC feedback control for wind and ESS hybrid power system frequency regulation," in *Proc. IEEE Power Electron. Mach. Wind Appl.*, Jul. 2012, pp. 1–7.
[24] H. Liu, Z. Hu, Y. Song, and J. Lin, "Decentralized vehicle-to-grid control for primary frequency regulation considering charging demands," *IEEE Trans. Power Syst.*, vol. 28, no. 3, pp. 3480–3489, Aug. 2013.
[25] Y. Ota, H. Taniguchi, T. Nakajima, K. M. Liyanage, J. Baba, and A. Yokoyama, "Autonomous distributed V2G (vehicle-to-grid) satisfying scheduled charging," *IEEE Trans. Smart Grid*, vol. 3, no. 1, pp. 559–564, Mar. 2012.
[26] H. Mahmood, D. Michaelson, and J. Jiang, "Decentralized power management of a PV/battery hybrid unit in a droop-controlled islanded microgrid," *IEEE Trans. Power Electron.*, vol. 30, no. 12, pp. 7215–7229, Dec. 2015.
[27] X. Lu, K. Sun, J. M. Guerrero, J. C. Vasquez, and L. Huang, "State-of-charge balance using adaptive droop control for distributed energy storage systems in DC microgrid applications," *IEEE Trans. Ind. Electron.*, vol. 61, no. 6, pp. 2804–2815, Jun. 2014.
[28] X. Lu, K. Sun, J. M. Guerrero, J. C. Vasquez, and L. Huang, "Double-quadrant state-of-charge-based droop control method for distributed energy storage systems in autonomous DC microgrids," *IEEE Trans. Smart Grid*, vol. 6, no. 1, pp. 147–157, Jan. 2015.
[29] C. Gavriluta, J. I. Candela, J. Rocabert, A. Luna, and P. Rodriguez, "Adaptive droop for control of multiterminal DC bus integrating energy storage," *IEEE Trans. Power Del.*, vol. 30, no. 1, pp. 16–24, Feb. 2015.
[30] J. W. Shim, Y. Cho, S.-J. Kim, S. W. Min, and K. Hur, "Synergistic control of SMES and battery energy storage for enabling dispatchability of renewable energy sources," *IEEE Trans. Appl. Supercond.*, vol. 23, no. 3, Jun. 2013, Art. no. 5701205.
[31] P. Wang, J. Xiao, and L. Setyawan, "Hierarchical control of hybrid energy storage system in DC microgrids," *IEEE Trans. Ind. Electron.*, vol. 62, no. 8, pp. 4915–4924, Aug. 2015.
[32] J. Pahasa and I. Ngamroo, "PHEVs bidirectional charging/discharging and SoC control for microgrid frequency stabilization using multiple MPC," *IEEE Trans. Smart Grid*, vol. 6, no. 2, pp. 526–533, Mar. 2015.
[33] H. Liu, Z. Hu, Y. Song, J. Wang, and X. Xie, "Vehicle-to-grid control for supplementary frequency regulation considering charging demands," *IEEE Trans. Power Syst.*, vol. 30, no. 6, pp. 3110–3119, Nov. 2015.
[34] J. Tan and Y. Zhang, "Coordinated control strategy of a battery energy storage system to support a wind power plant providing multi-timescale frequency ancillary services," *IEEE Trans. Sustain. Energy*, vol. 8, no. 3, pp. 1140–1153, Jul. 2017.
[35] B. M. Gundogdu, S. Nejad, D. T. Gladwin, M. P. Foster, and D. A. Stone, "A battery energy management strategy for U.K. Enhanced frequency response and triad avoidance," *IEEE Trans. Ind. Electron.*, vol. 65, no. 12, pp. 9509–9517, Dec. 2018.
[36] K. Das, M. Altin, A. D. Hansen, and P. E. Sørensen, "Inertia dependent droop based frequency containment process," *Energies*, vol. 12, no. 9, p. 1648, 2019. [Online]. Available: https://www.mdpi.com/1996-1073/12/9/1648
[37] O. Tremblay and L.-A. Dessaint, "Experimental validation of a battery dynamic model for EV applications," *World Electr. Vehicle J.*, vol. 3, no. 2, pp. 289–298, 2009.
[38] C. M. Shepherd, "Design of primary and secondary cells II. An equation describing battery discharge," *J. Electrochem. Soc.*, vol. 112, pp. 657–664, Jul. 1965.
[39] P. Kundur, *Power System Stability and Control* (The EPRI Power System Engineering Series). New York, NY, USA: McGraw-Hill, 1994.
[40] B. Kuo and F. Golnaraghi, *Automatic Control Systems*, 9th ed. New York, NY, USA: Wiley, 2009.
[41] M. Wright and P. Hearps, "Zero carbon Australia stationary energy plan," Melbourne Energy Inst., Univ. Melbourne, Melbourne, VIC, Australia, Tech. Rep., Aug. 2011.
[42] "100 per cent renewables study-modelling outcomes," Austral. Energy Market operator (AEMO), Tech. Rep., July 2013.

JAE WOONG SHIM (S'13–M'17) received the Ph.D. degree in electrical engineering jointly from Yonsei University, Seoul, South Korea, and The University of Sydney, Sydney, NSW, Australia, in 2016. His industry experience includes FACTS/HVDC control and operation as a Senior Researcher at the HVDC Research Center, LS Industrial Systems, from 2016 to 2017. He has been with the Department of Energy Engineering, Inje University, South Korea, since 2017, and currently leads the Electrical Power System Laboratory. His research interests include power system dynamics and control, HVDC/FACTS/ESS operation, multiterminal HVDC and MVDC, integration of renewable energy sources, and the interfaces of power electronics devices on power systems.

GREGOR VERBI (S'98–M'03–SM'10) received the B.Sc., M.Sc., and Ph.D. degrees in electrical engineering from the University of Ljubljana, Ljubljana, Slovenia, in 1995, 2000, and 2003, respectively. In 2005, he was a NATO-NSERC Postdoctoral Fellow with the University of Waterloo, Waterloo, ON, Canada. Since 2010, he has been with the School of Electrical and Information Engineering, The University of Sydney, Sydney, NSW, Australia. His expertise is in power system operation, stability and control, and electricity markets. His current research interests include grid and market integration of renewable energies and distributed energy resources, future grid modeling and scenario analysis, wide-area coordination of distributed energy resources, and demand response. He was a recipient of the IEEE Power and Energy Society Prize Paper Award, in 2006. He is an Associate Editor of the IEEE TRANSACTIONS ON SMART GRID.

HEEJIN KIM (S'10–M'15) received the B.S. and Ph.D. degrees in electrical engineering from Yonsei University, Seoul, South Korea, in 2010 and 2015, respectively. He was a Postdoctoral Fellow with Yonsei University, from 2015 to 2019. Since 2019, he has been with Yonsei University as a Research Professor. His research interests include modeling and control of power converters, modular multilevel converters, flexible ac transmission systems/high voltage direct current, power electronic applications in power systems, and integration of renewable energy.

KYEON HUR (S'04–M'07–SM'12) received the B.S. and M.S. degrees in electrical engineering from Yonsei University, Seoul, South Korea, in 1996 and 1998, respectively, and the Ph.D. degree in electrical and computer engineering from The University of Texas at Austin, Austin, TX, USA, in 2007. He was a Research and Development Engineer with Samsung Electronics, Suwon, South Korea, from 1998 to 2003. His industrial experience includes the Electric Reliability Council of Texas, Taylor, TX, USA, as a Grid Operations Engineer, from 2007 to 2008. He was also with the Electric Power Research Institute, Palo Alto, CA, USA, and conducted and managed research projects in grid operations and planning, from 2008 to 2010. He joined Yonsei University, in 2010, and since then, he has led a smart-grid research group. His current research interests include flexible ac transmission systems/high-voltage direct current, power system dynamics and control, and the integration of variable generation and controllable loads.